GENERIC ACTIVE DAMPING AND POINTING INTERFACE BASED ON A STEWART PLATFORM

2 authors:

Ahmed Mohammed Abu Hanieh
Birzeit University
30 PUBLICATIONS **229** CITATIONS
SEE PROFILE

A. Preumont
Université Libre de Bruxelles
246 PUBLICATIONS **3,323** CITATIONS
SEE PROFILE

GENERIC ACTIVE DAMPING AND POINTING INTERFACE BASED ON A STEWART PLATFORM

Ir. A. Abu Hanieh, Prof. A. Preumont
Université Libre de Bruxelles
50 Av. F. D. Roosevelt, 1050 Bruxelles, CP165/42, Belgium.
Tel: +32 (2) 650 26 87, Fax: +32 (2) 650 46 60
Dr. N. Loix
Micromega Dynamics sa,
Rue des Chasseurs Ardennais, 4301 Angleur, Belgium.
Tel: +32 (4) 365 23 63, Fax: +32 (4) 365 23 46

Abstract

This paper discloses a stiff active interface wherein a six degree of freedom Stewart platform, a standard hexapod with a cubic architecture, is used to actively increase the structural damping of flexible systems attached to it. It can also be used to rigidly connect arbitrary substructures while damping them. Each leg of the active interface consists of a linear piezo electric actuator, a collocated force sensor and flexible tips for the connections with the two end plates. By providing the legs with strain or elongation sensors, this active interface can also be used as an interface with infinite stiffness at low frequency (i.e. for machine tools), a 6 d.o.f. positioning and steering device for space applications as well as a microvibration isolator. The translation and rotation strokes of the interface are 90, 103 and 95 μm in the *x*, *y* and *z* directions respectively and 1300, 1150 and 700 μrad around the *x*, *y* and *z* directions respectively.

1. Introduction

Future astronometric missions will require improved angular resolution capabilities that are at least one order of magnitude better than the Hubble Space Telescope (0.05 μrad). This required angular resolution can only be achieved with either very large optics or interferometric devices, where the signals coming from several independent telescopes are combined to increase the global resolution. Space constraints such as weight or launcher size make interferometric devices attractive despite their increased complexity. To achieve the predicted resolution, the pointing error requirement of the individual telescopes is as low as a few nanoradians and their relative position must be preserved within a few nanometers. Usually, the optical path difference between the various sub-systems is monitored by a sophisticated laser metrology system and controlled by means of optical delay lines.

One concept for future space interferometers consists in mounting the various telescopes on a truss whose dimensions can be very large (i.e. 50-250m for IRSI-DARWIN). Because of the space constraints, this truss will be very flexible and subjected to a wide variety of static and dynamic perturbations (thermal loads, attitude control, reaction-wheels, cryo-coolers...). As the optical delay lines will compensate static and quasi-static perturbations, the main requirement on the supporting truss is rather stability than precision. This specification on the structural stability for scientific space missions has triggered extensive researches in the area of the active damping of flexible structures. These have led to numerous solutions, most of them based on the integration of SMART actuators and sensors in the structure itself. Several methods have been investigated by the present authors for the active damping of space structures:

- Replacing some bars of the truss by active struts [16].
- Integrating laminar piezo-electric patch [17]
- Using inertial actuators [18]
- Using active tendons [6]

In this paper, a stiff active damping interface is proposed. It can be used either as a support for payloads or to connect arbitrary substructures. It has the ability to introduce damping in the mechanical system attached to it while remaining stiff. The active interface consists of a six-degree of freedom Stewart platform, a standard hexapod with a cubic architecture. Each leg of the active interface is made of a linear piezo electric actuator, a collocated force sensor and flexible tips for the connection with the two end plates. The control architecture is based on six local/decentralized Integral Force Feedback controllers. By providing the legs with strain or elongation sensors, this active interface can also be used as an interface with infinite stiffness at low frequency (i.e. for machine tools), a 6 d.o.f. positioning and steering device for space applications as well as a microvibration isolator.

2. Assembly of the interface

The design of the proposed Stewart platform is based on the cubic configuration [2]. The dexterity and accuracy of the mechanism depends very much on the nominal geometry of the hexapod [14, 9]. The mobility of the platform is driven by the elongation of the legs [12, 13].

As far as the elongation of the legs in this application is very small, the kinematics configuration remains almost unchanged. Thus the Jacobian matrix that relates the motion of the platform to the elongation of the legs remains constant and can be evaluated from the nominal configuration depending only on the length of the legs [15]. To achieve good performances in active vibration damping and precision pointing, several characteristics should be taken into account in the design of the Stewart platform:

- Uniformity of control capability in all directions.
- Uniform stiffness in all directions.
- Uniform cross-coupling amongst actuators.
- Simple kinematics and dynamic analysis.
- Simple mechanical design.
- Availability of collocated actuator/sensor pairs.

The cubic configuration was invented by the Intelligent Automation Inc. (IAI) to fulfill most of the above properties [2]. The nominal configuration is obtained by cutting a cube by two planes as indicated in Fig.1. The two planes constitute both the base and the mobile plates of the Stewart platform. The edges of the cube connecting the plates represent the six legs of the hexapod.

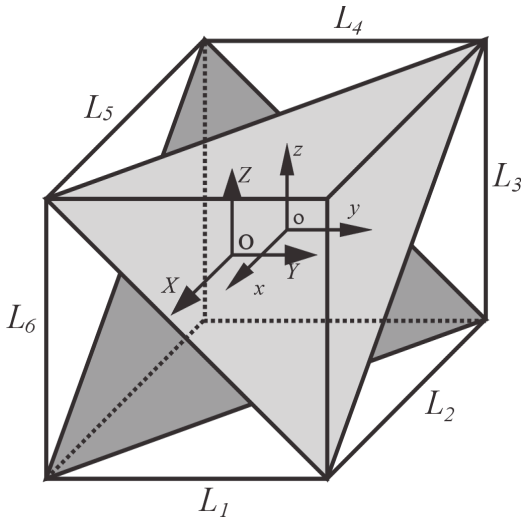

Figure 1: Cubic configuration of Stewart platform

From Fig.1, one can see that this Stewart platform is symmetrical in its nominal configuration and all legs are identical. Referring to the reference axes X, Y, Z (parallel to the legs) shown in Fig.1, the adjacent legs are orthogonal to each others resulting in a decoupled control action in the three translations X, Y and Z such that each two parallel legs control the translation in the parallel direction. This feature leads to a maximum uniformity of control authority in all directions. Note that in the analysis of the interface we use different reference axes where the XY-plane is parallel to the plane of the plates as shown in Fig.5.

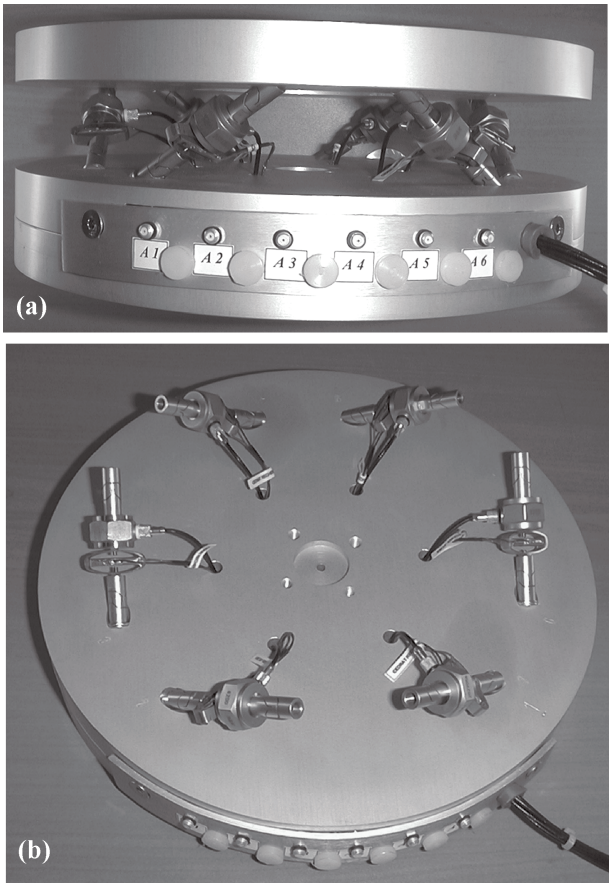

Figure 2: The Stewart platform (a): complete hexapod, (b): the hexapod with the upper plate removed

Fig.2(a) shows a picture of the complete Stewart platform and Fig.2(b) shows the same but with removing the upper plate. The two plates are circular aluminum plates with a thickness of 20 mm and a diameter of 250 mm. The plates are connected to each other by six active legs; the legs are mounted in such a way to achieve the geometry of cubic configuration (as explained before). Each active leg consists of a force sensor (B&K 8200) and an amplified piezoelectric actuator (Cedrat Recherche APA50s) as shown in Fig.3. To avoid the problems of friction and backlash in the joints, flexible tips were used instead of spherical joints. These flexible tips have zero friction, zero backlash, high axial stiffness and relatively low bending stiffness. It will be shown that the existence of this bending stiffness makes a limitation for the control authority because it shifts the transmission zeros to a higher frequency, which will decrease the damping effect expected from each closed-loop pole.

3. Kinematics and performance

Consider the schematic diagram shown in Fig.5 that represents the nominal configuration of the Stewart platform. Fig.5(a) is the cross-section through the XZ-plane and Fig.5(b) shows the top view of the hexapod; the two triangles here connect the points of anchorage of the legs on the two plates. The overall length of the

leg L is the basic parameter out of which all the kinematics are calculated:

$$L = l + \frac{2e}{\sin\theta} \tag{1}$$

where l is the nominal length of the leg assembly that equals to 66 mm (shown in Fig.3), e is the thickness of one platform. The two thicknesses are identical and equal to 20 mm. θ is the nominal inclination angle of the leg in the vertical plane including the leg and equals to 35.26 degrees. r is the distance from the center of the plate to the point of intersection of two adjacent legs; from geometry:

$$r^2 = L^2 - Z^2 \tag{2}$$

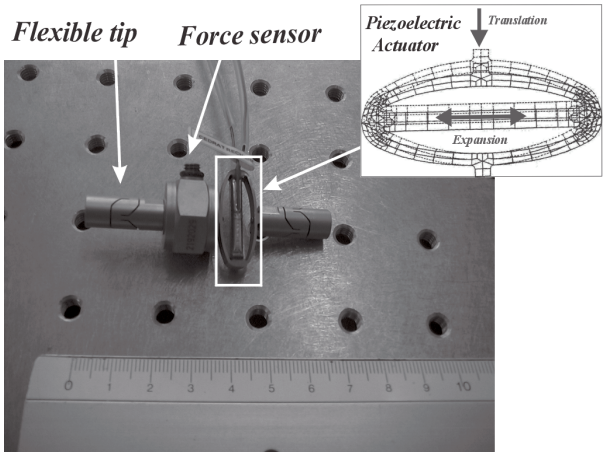

Figure 3: The active leg assembly of Stewart platform

This leads to the following relations:

$$\frac{r}{L} = \cos\theta = \sqrt{\frac{2}{3}}$$
$$\frac{Z}{L} = \sin\theta = \sqrt{\frac{1}{3}}$$

To estimate the Jacobian matrix that relates the elongation of the legs to the motion of the platform, let's consider the vectorial representation of the hexapod shown in Fig.4 where the notations are:

$\{B\}$ ≡ inertial reference frame of the lower platform (assumed fixed).
$\{P\}$ ≡ reference frame at the geometric center C of the top platform.
r_i ≡ position of the extremity of leg i in the lower platform, expressed in $\{B\}$.
p_i ≡ position of the extremity of leg i in the upper platform, expressed in $\{P\}$.
x_o ≡ the vector connecting the origin of $\{B\}$ to that of $\{P\}$, expressed in $\{B\}$.
1_i ≡ unit vector along leg i, expressed in $\{P\}$

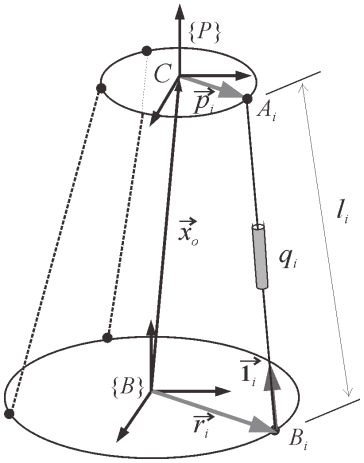

Figure 4: Vectorial representation of the Stewart platform

R is the rotation matrix relating $\{P\}$ to $\{B\}$, defined in terms of *roll/pitch/yaw* angles: $\boldsymbol{\theta}=(\gamma, \beta, \alpha)^T$.
The relationship between $\{B\}$ and $\{P\}$ is completely defined by x_o and $\boldsymbol{\theta}$, the Jacobian J relates the elongation velocities of the legs, $\dot{q}_i$, to the velocity vector $\dot{\chi} = (\mathrm{v}^T, \omega^T)^T$, where $\mathrm{v} = \dot{\mathrm{x}}_o$ and $\omega = \dot{\theta}$.

$$\dot{q} = J\dot{\chi} \tag{3}$$

The analytical expression can be obtained by expressing the absolute velocity $\vec{\mathrm{v}}_i$ of the extremity A_i (the extremity B_i is fixed in the inertial reference frame $\{B\}$, and projecting it along $\vec{1}_i$, we get

$$\vec{\mathrm{v}}_i = \vec{\mathrm{v}} + \vec{\omega} \times \vec{\mathrm{p}}_i \tag{4}$$

where $\vec{\mathrm{v}}$ is the absolute velocity of C and $\vec{\omega}$ is the angular velocity of the upper plate.

$$\begin{aligned} \dot{q}_i &= \vec{1}_i \cdot (\vec{\mathrm{v}} + \vec{\omega} \times \vec{\mathrm{p}}_i) \\ \dot{q}_i &= \vec{1}_i \cdot \vec{\mathrm{v}} - \vec{1}_i \cdot \vec{\mathrm{p}}_i \times \vec{\omega} \end{aligned} \tag{5}$$

and, upon projecting in the reference frame $\{P\}$,

$$\dot{q}_i = 1_i^T \mathrm{v} - 1_i^T \tilde{\mathrm{p}}_i \omega$$

where we have used the anti-symmetric matrix $\tilde{\mathrm{p}}_i$ to express the cross product $\mathrm{p}_i \times \omega = \tilde{\mathrm{p}}_i \omega$.
The above equation constitute the i^{th} line of the Jacobian:

$$\dot{\mathrm{q}} = J\dot{\chi} = \begin{pmatrix} \cdots & \cdots \\ 1_i^T & -1_i^T \tilde{\mathrm{p}}_i \\ \cdots & \cdots \end{pmatrix} \begin{pmatrix} \mathrm{v} \\ \omega \end{pmatrix} \tag{6}$$

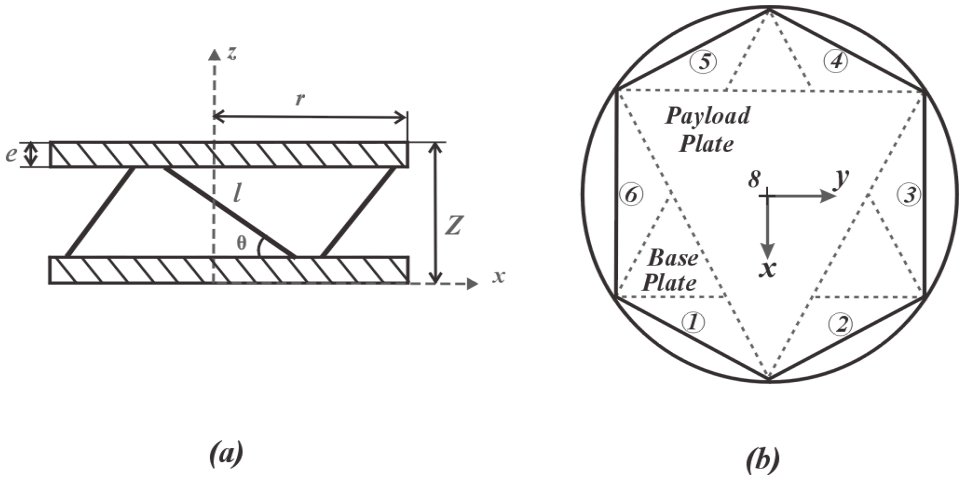

Figure 5: Schematic drawings of Stewart platform, (a): side section, (b): top view.

If v and ω are expressed in the moving frame $\{P\}$,

$$1_i = \frac{1}{l_i}\left[R^T\left(\mathrm{x}_o - \mathrm{r}_i\right) + \mathrm{p}_i\right]$$

where it has been assumed that x_o and r_i are expressed in $\{B\}$. It follows that

$$-1_i^T \tilde{\mathrm{p}}_i = -\frac{1}{l_i}\left(\mathrm{x}_o - \mathrm{r}_i\right)^T R\tilde{\mathrm{p}}_i$$

The velocity Jacobian matrix becomes

$$J = \begin{pmatrix} \cdots & \cdots \\ \frac{1}{l_i}\left[\left(\mathrm{x}_o - \mathrm{r}_i\right)^T R + \mathrm{p}_i^T\right] & \frac{1}{l_i}\left(\mathrm{x}_o - \mathrm{r}_i\right)^T R\tilde{\mathrm{p}}_i \\ \cdots & \cdots \end{pmatrix} \qquad (7)$$

The force Jacobian can be obtained from the virtual work theorem,

$$\mathrm{f}^T \delta\mathrm{q} = \mathrm{f}^T J \delta\chi = \left(\mathrm{F}^T, \mathrm{T}^T\right)\delta\chi$$

where f stands for the forces along the legs of the platform and F and T are respectively the resultant force and the resultant torque applied to the upper platform. It follows that **F** and T, expressed in the same reference frame as **v** and ω, are related to the forces acting in the leg **f** by:

$$\begin{pmatrix} \mathrm{F} \\ \mathrm{T} \end{pmatrix} = B\mathrm{f} \qquad (8)$$

where $B=J^{\mathrm{T}}$ is the force Jacobian and equals to:

$$B = \begin{pmatrix} \cdots & 1_i & \cdots \\ \cdots & \tilde{\mathrm{p}}_i 1_i & \cdots \end{pmatrix} \qquad (9)$$

or

$$B = \begin{pmatrix} \cdots & \frac{1}{l_i}\left[R^T\left(\mathrm{x}_o - \mathrm{r}_i\right)^T + \mathrm{p}_i\right] & \cdots \\ \cdots & \frac{1}{l_i}\tilde{\mathrm{p}}_i R^T\left(\mathrm{x}_o - \mathrm{r}_i\right) & \cdots \end{pmatrix}$$

The Jacobian matrix allows transforming the pointing control requirements (in terms of $\delta\chi$) into length requirements δq of the platform legs. This decoupling transformation produces 6 independent actuator commands for the individual legs. For a length of the leg equals to 135.3 mm (the overall nominal leg length) the velocity Jacobian in numerical values can be given as:

$$J = \begin{pmatrix} 0.408 & 0.707 & 0.577 & 0 & -0.064 & 0.078 \\ 0.408 & -0.707 & 0.577 & 0 & -0.064 & -0.078 \\ -0.816 & 0 & 0.577 & 0.055 & 0.032 & 0.078 \\ 0.408 & 0.707 & 0.577 & 0.055 & 0.032 & -0.078 \\ 0.408 & -0.707 & 0.577 & -0.055 & 0.032 & 0.078 \\ -0.816 & 0 & 0.577 & -0.055 & 0.032 & -0.078 \end{pmatrix}$$

Neglecting the bending stiffness of the flexible tips in the legs, we find that the general stiffness matrix of the hexapod $K = BK_l B^T = J^T K_l J$, where $K_l = 0.87\ 10^6$N/m is the axial stiffness of each leg. The stiffness is calculated numerically and is equal to

$$K = 10^6 \begin{pmatrix} 1.74 & 0 & 0 & 0 & -0.068 & 0 \\ 0 & 1.74 & 0 & 0.068 & 0 & 0 \\ 0 & 0 & 1.74 & 0 & 0 & 0 \\ 0 & 0.068 & 0 & 0.0106 & 0 & 0 \\ -0.068 & 0 & 0 & 0 & 0.0106 & 0 \\ 0 & 0 & 0 & 0 & 0 & 0.0319 \end{pmatrix}$$

The maximum stroke of the actuator is 55 μm (±27.5 μm) but this motion is magnified by the mechanism of the Stewart platform to give the motion of the mobile plate. This fact can be an important advantage for pointing purposes.

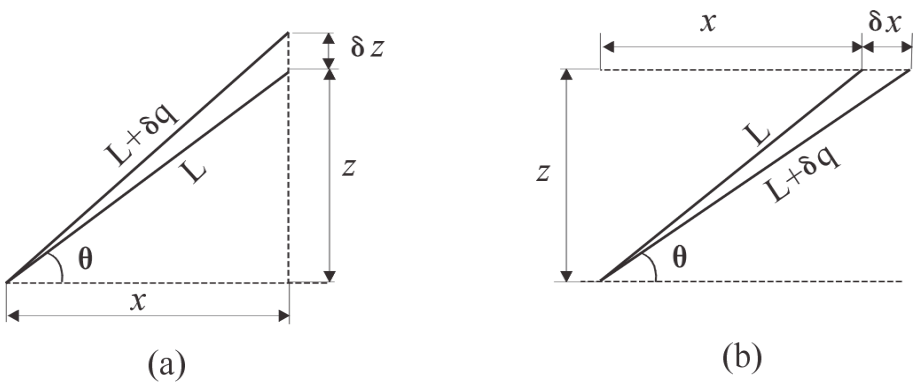

Figure 6: Leg configurations for performance calculation (a): deformation of the leg to give pure motion in the z-direction, (b): deformation of legs 3 and 6 to give pure motion in the x-direction

Consider moving the mobile plate in a pure piston motion in the z-direction; in this case all the actuators will elongate with the same length as shown in Fig.6(a). We can calculate analytically the relation between the elongation of the leg δq and the motion in the z-direction δz; from trigonometric analysis:

$$x^2 = L^2 - z^2 = (L + \delta q)^2 - (z + \delta z)^2$$

This leads to the relation:

$$\delta z = \sqrt{3}\delta q \qquad (10)$$

In the same way, when one needs to move the platform in a pure motion in the x-direction, the legs 3 and 6 will elongate as shown in Fig.6(b) to define this motion. This motion in x-direction is limited by the full stroke of legs 3 and 6 but it is also accompanied by a half-stroke elongation of the other four legs. Applying the trigonometric relations again we find:

$$z^2 = L^2 - x^2 = (L + \delta q)^2 - (x + \delta x)^2 \qquad (11)$$

This leads to the relation:

$$\delta x = \sqrt{\frac{3}{2}}\delta q \qquad (12)$$

The pure rotational motion is defined by the ratio between the elongation δq and the nominal length of the leg L. In the case of a pure rotation around the x-axis, the following relation defines the rotated angle $\delta\theta_x$:

$$\delta\theta_x = \sqrt{6}\frac{\delta q}{L} \qquad (13)$$

The pure rotation around the x-axis results from the pure positive motion of the legs 3 and 4 in the z-direction accompanied with a pure negative motion of the legs 5 and 6 in the z-direction or vice versa while legs 1 and 2 stay still. On the other hand, to get a pure rotation around the z-axis, all the legs should elongate in the way shown in Fig.6(b) but in alternative way (e.g. legs 1,3 and 5 make a positive motion and legs 2,4 and 6 make a negative motion or vice versa). The rotation angle around the z-axis is related to the absolute elongation of one leg as follows:

$$\delta\theta_z = \frac{3}{2}\frac{\delta q}{L} \qquad (14)$$

Table 1 shows the maximum pure translations and rotations in the different degrees of freedom. The total stroke of the piezo actuator is 55 μm, for symetric operations, the maximum stroke of the actuator s = ±27.5 μm. δq_i is the elongation in the i^{th} leg given in μm and DOFs are the maximum pure translations (in μm) and rotations (in μrad) travelled by the center of the upper plate.

DOFs	δq_1	δq_2	δq_3	δq_4	δq_5	δq_6
x_{pure} = 33.7	s/2	s/2	-s	s/2	S/2	-s
y_{pure} = 38.9	s	-s	0	s	-s	0
z_{pure} = 47.5	s	s	s	s	s	s
θ^x_{pure} = 498	0	0	s	s	-s	-s
θ^y_{pure} = 431	-s	-s	S/2	s/2	s/2	s/2
θ^z_{pure} = 350	s	-s	s	-s	s	-s

Table 1: Maximum pure translations (in μm) and rotations (in μrad) traveled by the moving plate and the corresponding leg configurations (s = ±27.5 μm)

The previous table shows the motions for the half-stroke of the actuator, which means that the full translations along x, y and z (in μm) and the rotations around them (in μrad), respectively, are (67, 79, 95, 996, 862, 700).

When the motion is a combination of several directions it becomes more complicated. A simple optimization technique has been used to calculate the different configurations that give the maximum motions in the six d.o.f of the platform. The maximum displacements values and the corresponding leg configurations are shown in Table 2. Note that the maximum motions shown here are not pure motions but they are coupled with other motions at the same time.

DOFs	δq_1	δq_2	δq_3	δq_4	δq_5	δq_6
x_{pure} = 45	-s	-s	-s	s	s	-s
y_{pure} = 51.5	s	-s	-s	s	-s	s
z_{pure} = 47.5	s	s	s	s	s	s
θ^x_{pure} = 650	-s	s	s	s	-s	-s
θ^y_{pure} = 575	-s	-s	-s	s	s	-s
θ^z_{pure} = 350	s	-s	s	-s	s	-s

Table 2: Maximum coupled translations (in μm) and rotations (in μrad) travelled by the moving plate and the corresponding leg configurations (s = ±27.5 μm)

Again, this table shows the motions for the half-strokes of the actuators and the full motions of the mobile plate is twice that; the full translations along *x*, *y* and *z* (in μm) and the rotations around them (in μrad) are (90, 103, 95, 1300, 1150, 700) respectively.

The signal to noise ratio of commercial power electronics for piezo actuators is about 80dB. As the position noise is linearly proportional to the electrical noise, the resolution of piezoelectric actuator is about 0.01% of its stroke. In present case, the piezo noise for a 55μm stroke actuator should be 5.5nm$_{rms}$. As the pointing commands in the hexapod are amplified and transferred into motion of the upper plate, the noise is also amplified. To find the RMS values of the noise on the platform, consider that

$$\delta x_i = \sqrt{\sum_j \left(J_{ij}^{-1}\right)^2 \delta q_j^2} \qquad (15)$$

where δx_i is the amplified noise in the i^{th} direction of motion of the platform, δq_j is the noise produced by the j^{th} leg and J_{ij} is the Jacobian value relating the previous two. Referring to the maximum translations and rotations moved by the platform due to the full strokes of the actuators (Table 2) and knowing that the maximum noise in each leg equals to 5.5 nm$_{rms}$, Table 3 gives the resolution of the platform.

DOFs	Resolution
x_{noise}	4.5 nm$_{rms}$
y_{noise}	5.2 nm$_{rms}$
z_{noise}	3.9 nm$_{rms}$
θ^x_{noise}	66.4 nrad$_{rms}$
θ^y_{noise}	57.5 nrad$_{rms}$
θ^z_{noise}	28.7 nrad$_{rms}$

Table 3: Resolution of the six degrees of freedom of the platform

4. Active damping

In order to evaluate the damping performances of the interface, the hexapod is connected to a flexible payload. The inertia matrix is defined by *M* and the general stiffness matrix is defined by *K*. The external forces and moments acting on the payload frame (upper plate) is expressed in the vector *F* [4]. The governing equation of motion in Laplace transform are:

$$Ms^2x + Kx = F \qquad (16)$$

As explained before, there is a force sensor located in each leg of the hexapod and collocated with the actuator. The function of this sensor is to measure the axial force resulting in that leg in order to feed the signal back to the actuator when the loop is closed. The sensor output equation becomes:

$$y = K_l(q - \delta)$$

Where $y = (y_1, ..., y_6)^T$ is the 6 force sensor outputs, $q = (q_1, ..., q_6)^T$ is the vector of leg extension from the equilibrium position, K_l is the strut stiffness and $\delta = (\delta_1, ..., \delta_6)^T$ is the vector of the 6 active control displacements of the piezo actuators; here $F = BK_l\delta$. Taking into account the relationship between the leg extensions and the payload frame displacements; $q=B^Tx$, we have:

$$y = K_l\left(B^Tx - \delta\right) \qquad (17)$$

Using the decentralized integral force feedback with constant gain *g*, the control law is:

$$\delta = \frac{g}{K_l s} y \qquad (18)$$

This leads to the closed-loop equation of motion:

$$Ms^2x + Kx = \frac{g}{s+g} BK_l B^T x \qquad (19)$$

or

$$\left[Ms^2 + K - \frac{g}{s+g} BK_l B^T\right]x = 0 \qquad (20)$$

In addition to the stiffness of the payload truss, the general stiffness matrix of the system also includes the axial stiffness and the bending stiffness of the hexapod legs. If there is no bending stiffness in the legs, the transmission zeros of the system ω_l (asymptotic solutions of the closed-loop equation as $g \to \infty$) are located at the origin since the system without piezo has rigid body modes. With a bending stiffness in the legs due to the flexible tips, these transmission zeros will be moved away from the origin: there will be no more rigid body mode to appear when the piezos are removed.

To transform Equ.(20) into modal coordinates, one may substitute by $x = \Phi z$ and, assuming that the mode shapes are normalized according to $\Phi^T M\Phi = I$ and that $\Phi^T K\Phi = \Omega^2$, Equ.(20) equation becomes:

$$\left[s^2 + \Omega^2 - \frac{g}{s+g}\Phi^T BK_l B^T\Phi\right]z = 0 \qquad (21)$$

From the analysis explained deeply in [4, 6] we have:

$$\Phi^T \left(BK_l B^T\right)\Phi \approx diag\left(\nu_i \Omega_i^2\right) \qquad (22)$$

where ν_i is the fraction of modal strain energy in the active legs when the structure vibrates according to mode *i*. It can be shown that the frequencies of the transmission zeros can be found from [4]:

$$\omega_i^2 = \Omega_i^2 \left(1 - \nu_i\right) \qquad (23)$$

In terms of these parameters, the characteristic equation can be written as

$$s^2 + \Omega_i^2 - \frac{g}{s+g}\left(\Omega_i^2 - \omega_i^2\right) = 0 \qquad (24)$$

or

$$1 + g\frac{\left(s^2 + \omega_i^2\right)}{s\left(s^2 + \Omega_i^2\right)} = 0 \qquad (25)$$

The transmission zeros (the solution of Equ.(20) as $g \rightarrow \infty$) are defined here by $\pm\omega_i$. This shift of the zeros from the origin has a substantial influence on the practical control performance of the Stewart platform.

5. Experimental results

To test the interface, a 150 cm long steel truss structure was attached on the upper plate of the hexapod (Fig.7). This system has been modeled using a Finite Element Model (SAMCEF) and the natural frequencies of the open-loop system Ω_i have been computed. Table 4 lists the first six modes showing the mode shapes and the frequencies.

Mode	Freq. (Hz)	Mode shape
1	3.82	Bending in the XZ-plane
2	4.21	Bending in the YZ-plane
3	45.35	Torsion around the Z-axis
4	65.62	Bending in the XZ-plane
5	78.97	Bending in YZ-plane
6	87.44	Translation in the Z-direction

Table 4: Frequencies and mode shapes taken from the finite element model

A decentralized integral force feedback control scheme was applied to the experimental system. The six independent controllers have been implemented on a DSP board. The six loops have been closed separately and, although the control loops were independent, the feedback gains used in all the loops are identical. Fig.8 presents some experimental results. The time response shows the signal from one of the force sensors located in the legs; the truss is subjected to an impulse at middle height, without then with control. The frequency responses (with and without control) are obtained between a perturbation signal applied to the piezo actuator of one the leg and its collocated force sensor.

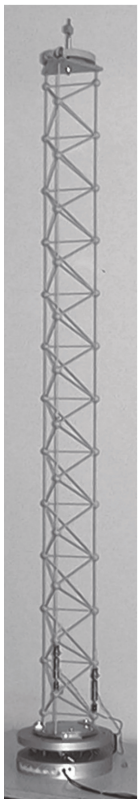

Figure 7: Experimental setup

On can see that fairly high damping ratios can be achieved for the low frequency modes (4-5Hz) but also significant damping in the high frequency modes (40-90Hz). Unfortunately, the results on the torsion mode have been disappointing, probably due to the flexion stiffness in the flexible tips. The experimental root locus for the first two modes is shown in Fig.9 and is compared to the estimated theoretical root locus, Ω_i and ω_i are the resonance and transmission zeros of the experimental FRF. It has been shown by FEM that ω_i are the resonance of the system where the axial stiffness of the legs has been set to zero.

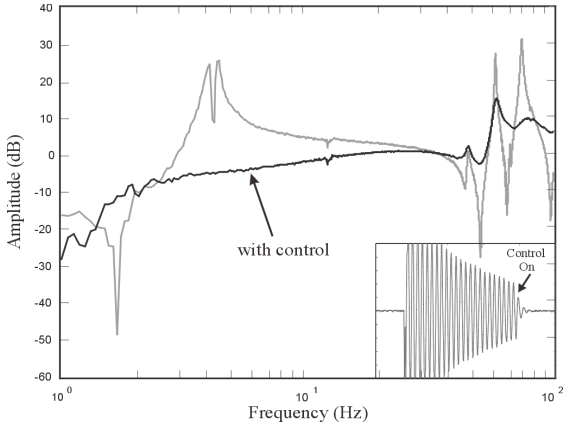

Figure 8: Experimental time response and frequency response function of the truss mounted on the active interface.

6. Conclusions

This paper describes a new generation of hard mount Stewart platform. Some terrestrial and spatial applications were discussed with deeper overview on the possibility of using such a device in the precise pointing and vibration suppression of the highly sensitive spatial equipment. The second part of this paper shows the design, assembly and configuration of the hexapod explaining the principle and advantages of the cubic configuration. The kinematics and pointing performance of the interface was discussed in the third section. Analytical and numerical analyses were established to show how the different degrees of freedom of the mobile plate are related to the elongation of the six legs of the hexapod. Part four concentrated on the dynamics and the theoretical relations of the applied control technique. Eventually, some experimental results were shown in the last section explaining the performance of the device in active vibration damping.

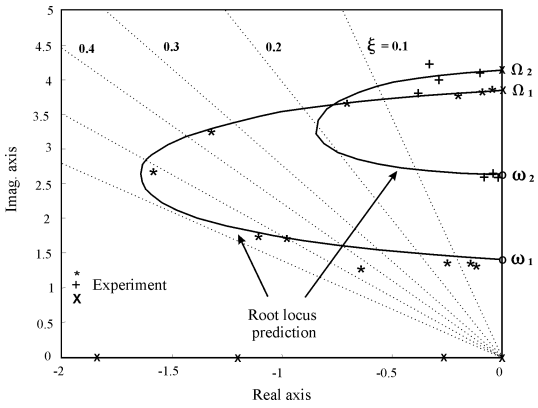

Figure 9: Experimental root locus compared to theoretical estimation

Acknowledgment

This work was supported by the Inter University Attraction Pole IUAP-IV-24 on Intelligent Mechatronics Systems.

Reference

[1] D. Stewart, A platform with six degrees of freedom, *Proc Instn Mech Engrs*, Vol.180 (15): 371-378, 1965 - 1966.

[2] Z.J. Geng and L.S. Haynes, Six degree-of-freedom active vibration control using the Stewart platforms, *IEEE Transactions on Control Systems Technology*, 2(1), 45 -- 53, March 1994.

[3] A. Preumont, Modular payload isolation mounts based on Stewart Platforms, *Draft report prepared in support of the GSTP proposal*, December, 1999.

[4] A. Preumont, *Vibration control of active structures*, 1st. ed., Kluwer Academic Publishers, 1997.

[5] W. Thomson, *Theory of vibration with applications*, 2nd ed. George Allen and Unwin, 1981.

[6] A. Preumont, Y. Achkire, F. Bossens, Active tendon control of Large trusses. *AIAA Journal*, vol. 38, No. 3, March 2000.

[7] E.I. Rivin, Principles and criteria of vibration isolation of machinery, *Transactions of the ASME, Journal of Mechanical Design*, Vol.101: 682 -- 692, October 1979.

[8] J.F.I.O'Brien, G.W.Neat, J.W.Melody, R.J. Calvet and A. von Flotow, Six-axis vibration isolation technology applied to spaceborne interferometers, *In Spaceborne Interferometry II (R.D. Reasenberg, ed.), proc. SPIE*, vol. 2447, Orlando FL., Apr. 1995.

[9] J. Craig, *Introduction to Robotics*, Addison-Wisley publishing company, 1986.

[10] J. Spanos, Z. Rahman, G. Blackwood, A Soft 6-axis Active Vibration Isolator, *Proceedings of the American Control Conference*, 412-416, June. 1995.

[11] G. Franklin, J.Powell and A.Emami-Naeini, *Feedback control of dynamic systems*, 3rd. ed., Addison-Wesley publishing company, 1994.

[12] J.P. Merlet, An algorithm for the forward kinematics of general parallel manipulators, *IEEE*, 1991.

[13] C. Reboulet and T. Berthomieu, Dynamic models of a six-degree of freedom parallel manipulators, ICAR'91, 1153-1157, Pisa, June 1991.

[14] K.H. Pittens and R.P. Podhorodeski, A family of Stewart platforms with optimal dexterity, *Journal of Robotic Systems*, 10(4), 463 - 479, December 1993.

[15] J.E.McInroy, J.F.O'Brien and G.W.Neat, Precise, fault-tolerant pointing using a Stewart platform, *IEEE/ASME Transactions on Mechatronics*, Vol.4, No 1, pp.91-95, March 1999.

[16] A. Preumont, J.P. Dufour and C. Malekian, Active damping by local force feedback with piezoelectric actuators, *AIAA / ASME*, SDM Conference, Baltimore, MD, April 1991. ESA 1st Conf. on Spacecraft, Guidance, Navigation and Control Systems, Noordwijk, June 1991.

[17] N. Loix and A. Preumont, Remarks on the modelling of active structures with colocated piezoelectric actuators and sensors, *ASME Conference on Mechanical Vibration and Noise*, Boston, September 1995.

[18] A. Preumont, N. Loix, D. Malaise and O. Lecrenier, Active Damping of Optical Test Benches with Acceleration Feedback, *Machine Vibration*, Vol 2, 119-124, 1993.